

# Applications of a Geiger-Müller Counter: Study of Range of Beta Particles, Attenuation of Bremsstrahlung and Back Scattering

Gayatri P

3rd year, Integrated M.Sc. Physics

Roll No.: 2211185

(Dated: April 15, 2025)

In this experiment, we investigate the performance of a Geiger-Muller counter using Tl-204 and Sr-90 beta sources. The half-thickness method is used to determine beta particle range and endpoint energy. We also explore Bremsstrahlung production and attenuation, beta backscattering, focusing on the effects of absorber material and thickness. These findings enhance understanding of beta radiation interactions and aid in optimizing radiation detection and shielding.

## I. THEORY

Beta decay is commonly observed in unstable nuclei that contain an excess of neutrons compared to protons. The  $\beta$  particles are typically high-energy electrons ( $\beta^-$ ) or positrons ( $\beta^+$ ) that are ejected from the nucleus. These particles have a much smaller mass than a proton, making up only onehalf of one-thousandth of its mass. Despite their small mass, they can achieve high speeds close to the speed of light due to their high energy.

Because of their light mass,  $\beta$  particles quickly lose energy as they interact with matter. As a result, they have limited ranges in materials, typically only a few millimeters. However, their range in air can be tens of centimeters, depending on their energy. The process of beta decay and the resulting beta radiation have important applications in various fields, including nuclear physics and medical imaging. The ability of  $\beta$  particles to penetrate materials to a limited depth makes them useful in measuring material thickness and in detecting material defects. In medicine, beta-emitting radioactive isotopes are used for cancer treatment and imaging.

### A. Range of $\beta$ particle

The maximum distance beta particles can travel within a material before losing all their energy and being completely absorbed is referred to as their range. This range depends on both the initial kinetic energy of the beta particles and the density of the material they traverse. The endpoint energy ( $E_0$ ) represents the highest kinetic energy a beta particle can have when emitted from a radioactive source, as beta decay results in a continuous energy spectrum. A widely used method for determining beta particle range is the half-thickness technique, which involves measuring the thickness of an absorber required to reduce the detected count rate by half.

The range of  $\beta$  particle is given by

$$R = (0.52E_0 - 0.09) \text{ g/cm}^2 \quad (1)$$

where  $E_0$  is the endpoint energy of the beta rays in MeV. The ratio of thickness required to reduce the counts of

beta rays from one source to half to the thickness required for the other source is given by

$$\frac{t_{\frac{1}{2},1}}{t_{\frac{1}{2},2}} = \frac{\text{Range of beta rays from first source}}{\text{Range of beta rays from second source}} \quad (2)$$

$$\frac{t_{\frac{1}{2},1}}{t_{\frac{1}{2},2}} = \frac{R_1}{R_2} \quad (3)$$

By comparing half-thickness values for different beta sources, the range for an unknown source can be estimated.

### B. Back scattering

When a  $\beta$  particle, either an electron or a positron, enters a material, it undergoes a series of interactions with the atoms in the material. The attractive electrostatic force between the positively charged nucleus of the atoms and the negatively charged  $\beta$  particle causes the path of the  $\beta$  particle to be deflected. The degree of deflection depends on the energy of the  $\beta$  particle, but the overall effect is a scattering of the particles. Typically, this causes the forward direction of the  $\beta$  particle to change by a few degrees.

In some cases, however, the angle of deflection can be quite large, and the  $\beta$  particle can be deflected back in the direction from which it came. This phenomenon is known as backscattering, and it occurs when the angle of deflection is greater than 90 degrees. Backscattering is more likely to occur in materials with high atomic number, as the larger number of positively charged nuclei increases the likelihood of a strong electrostatic interaction with the  $\beta$  particle.

Backscattering of  $\beta$  particles has important implications for radiation detection and measurement. For example, when using a detector to measure the amount of beta radiation emitted from a sample, backscattering can cause a portion of the radiation to be reflected back into the sample, leading to an overestimation of the true amount of radiation emitted. To mitigate this effect, detectors are often designed with thin windows or other

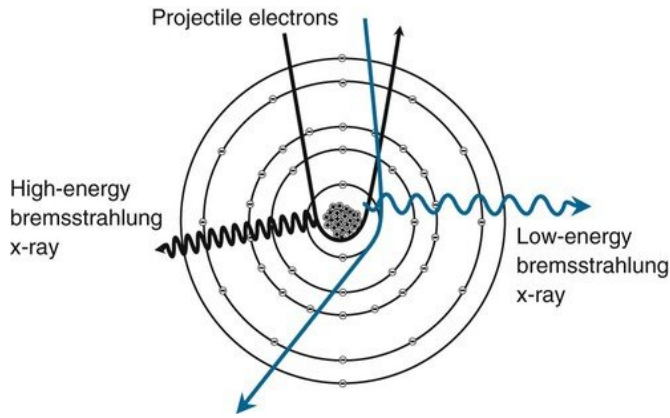


FIG. 1: Origin of Bremsstrahlung radiation

features that minimize backscattering and allow the  $\beta$  particles to escape from the sample more easily.

In addition to its impact on radiation detection, backscattering of  $\beta$  particles also plays a role in the interactions between radiation and matter in a variety of contexts, including medical imaging and radiation therapy. Understanding the principles of backscattering is therefore important for a wide range of applications in the fields of nuclear physics, radiation biology, and radiation protection.

### C. Bremsstrahlung Radiation

Bremsstrahlung is a form of electromagnetic radiation which is generated when a charged particle experiences a deceleration by another charged particle, such as an atomic nucleus. When a  $\beta$  particle moves through matter, it may encounter a nucleus and be deflected by it. This deflection causes a reduction in the  $\beta$  particle's kinetic energy, resulting in the emission of energy in the form of a photon of bremsstrahlung radiation or 'breaking radiation' (Fig. 1). The energy of the emitted bremsstrahlung photon is equal to the difference in energy between the initial and final kinetic energies of the  $\beta$  particle.

The amount of bremsstrahlung radiation emitted by a  $\beta$  particle depends on several factors, including the kinetic energy of the  $\beta$  particle, the atomic number of the absorbing material, and the density of the material. As the  $\beta$  particle approaches a nucleus and is deflected, the magnitude of the deflection and the associated energy loss depend on the proximity and atomic charge of the nucleus. The closer the  $\beta$  particle is to the nucleus, the greater the energy loss, and the higher the frequency of the emitted bremsstrahlung photons. In addition, the higher the atomic number of the absorbing material, the greater the number of potential nuclei that the  $\beta$  particle may interact with, leading to an increased probability of bremsstrahlung radiation emission.

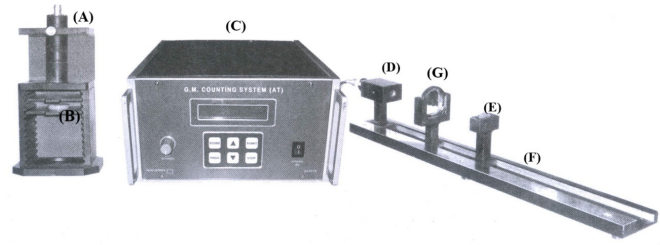


FIG. 2: Experimental Setup where (A) and (B) are the end window detector and source holder (C) is the GM counting system where you can vary the EHT (D) and (E) are the end window detector and source holders attached to a (F) sliding bench. (G) is the stand for the aluminium absorber set.

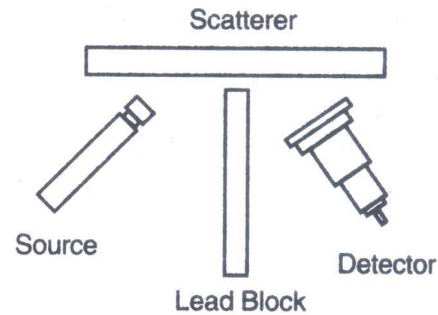


FIG. 3: Schematic diagram for the measurement of back-scattering

### Apparatus

1. Sr-90 and Th-204 samples
2. GM counting System
3. GM detector
4. Sliding Bench
5. Detector Stand
6. Aluminium Absorber set
7. Lead block for isolation
8. Absorber stand for back-scattering
9. Copper, Aluminium and Perspex plates
10. BNC cable

Fig. 2 shows and labels the used apparatuses in this experiment. Fig. 3 shows the schematic diagram of backscattering experiment.

## II. OBSERVATION AND CALCULATIONS

### A. Range of $\beta$ particles

For the measurement of the range of the  $\beta$  particles from Sr-90, first the half thickness is determined for a source whose range is known (Th-204). Then the half thickness is found out for Sr-90. From that the range and

Background Count (in 60s)	Average Count (in 60s)	Avg. Background CPS ( $s^{-1}$ )
54	56	0.933
53		
72		
53		
48		

TABLE I: Background counts measured for the beta detector

Absorber thickness (mm)	Tl-204 Count (in 180s)	Tl-204 CPS ( $s^{-1}$ )	Sr-90 Count (in 100s)	Sr-90 CPS ( $s^{-1}$ )
0.00	6946	37.656	6191	60.977
0.06	5336	28.711	5244	51.507
0.12	3935	20.928	4652	45.587
0.18	3106	16.322	4231	41.377
0.24	2419	12.506	3763	36.697
0.30	1731	8.683	3442	33.487
0.36	1374	6.700	3282	31.887
0.42	1002	4.633	3058	29.647
0.48	608	2.444	2799	27.057
0.54			2661	25.677
0.60			2570	24.767

TABLE II:  $\beta$  counts observed for both Tl-204 and Sr-90 with varying levels of absorber thickness. The CPS values are corrected based on Table I

end point energy of the  $\beta$  particles can be found.

During this part of the experiment, the EHT voltage is fixed to 480 V. Distance of source to the detector is 3 cm and distance of absorber to the detector is 2 cm.

Table I shows the background CPS measured for the setup. Table II shows the  $\beta$  counts obtained from the detector for both the sources with varying absorber thicknesses.

Fig. 4 and 5 show the plots for  $\beta$  CPS vs. surface density of Al, for both the sources respectively. The surface density of Al was calculated as  $\rho \times \text{thickness}$ , where  $\rho = 2.71 \text{ g/cm}^3$  is the volume density.

We have fitted an exponential curve to the count vs. surface density data and have observed that the surface density at half the initial CPS is  $t_{\frac{1}{2}, \text{Tl}} = 39.84 \text{ mg/cm}^2$  and  $t_{\frac{1}{2}, \text{Sr}} = 105.69 \text{ mg/cm}^2$ .

Using the known end-point energy of Tl-204 as 0.764 MeV, we can calculate  $R_{\text{Tl}} = 0.307 \text{ g/cm}^2$  using Eq. 1. Now, plugging these in Eq. 2, we get,

$$R_{\text{Sr}} = R_{\text{Tl}} \left( \frac{t_{\frac{1}{2}, \text{Sr}}}{t_{\frac{1}{2}, \text{Tl}}} \right) = 0.826 \text{ g/cm}^2$$

Plugging this back into Eq. 1, we get the end-point energy of Sr-90 to be  $E_0 = 1.761 \text{ MeV}$ .

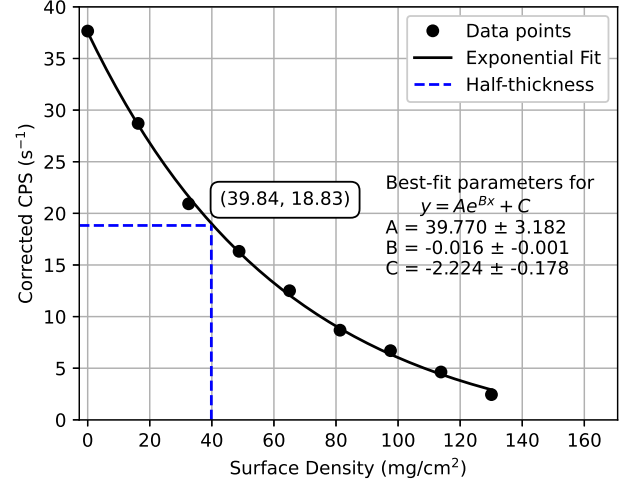


FIG. 4: CPS vs. Surface charge density plot for Tl-204

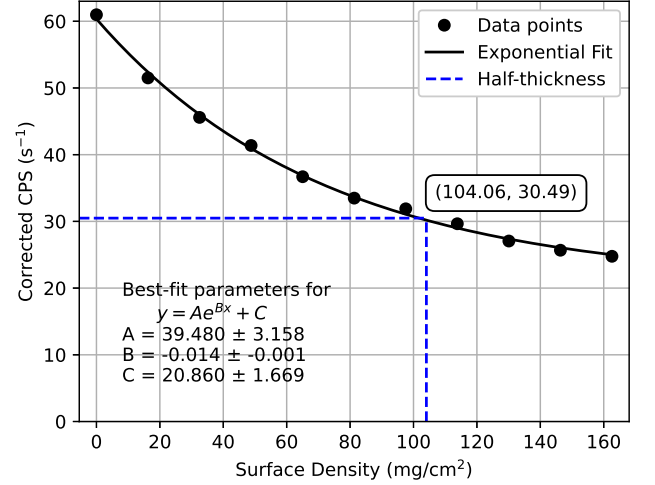


FIG. 5: CPS vs. Surface charge density plot for Sr-90

## B. Attenuation of Bremsstrahlung

For measuring the bremsstrahlung effect, the source and the detector are kept at a fixed distance (6cm) and then the combinations of absorber plates are put in between them. Tables III shows the count rates with different combinations of absorbers in different positions.

EHT voltage is 480V. The counts are recorded for 180s each.

As we can see, the bremsstrahlung count rate is influenced by the arrangement of absorbent materials. If a metal sheet is positioned closest to the source, a higher count rate is recorded because bremsstrahlung is produced in the aluminum but minimally absorbed by the following Perspex sheet. Conversely, if the  $\beta$  rays first pass through a plastic sheet, the resulting bremsstrahlung

for Al and perspex			
Sl. No.	Absorber	Count	Corrected Count
1	No Absorber	5662	5418
2	Al Facing	611	367
3	Perspex Facing	571	327

for Al and copper			
Sl. No.	Absorber	Count	Corrected Count
1	No Absorber	5662	5418
2	Al Facing	373	129
3	Copper Facing	456	212

for Copper and Perspex			
Sl. No.	Absorber	Count	Corrected Count
1	No Absorber	5662	5418
3	Copper Facing	436	192
2	Perspex Facing	398	154

TABLE III: Bremsstrahlung data. Each count is for 300s each. The avg. background count was measured to be 244 (from three measurements of 249, 243 and 240).

has lower energy, and a significant portion is absorbed by the subsequent metal sheet. For the Al+Cu combination, we find that the count rate is lower when Al is facing the source. This is because the atomic number of Al ( $Z = 13$ ) is lower than that of Cu ( $Z = 29$ ). This means there is a higher amount of bremsstrahlung produced in Cu as the  $\beta$  particles experience more nuclear force.

### C. Backscattering of $\beta$ particles

To measuring the backscattering radiation, the source and detector are separated by a lead block and they both face the aluminium scatterer, at an angle of  $90^\circ$  with each other. The thickness of the Aluminium scatterer is varied and recorded in Table IV. Fig. 6 shows the count vs. thickness of Al plot.

From Fig. 6, we can observe that the counts due to back-scattering increases upto a certain thickness of the scatterer and then more or less stabilizes. From this the saturation thickness of the Al can be approximated to be approximately 0.35 mm.

## III. ERROR ANALYSIS

For the first part the uncertainty in  $R_{Sr}$  can be calculated using the error propagation methods on Eq. 2. For that we know that the uncertainty in thickness of the Al is 0.01 mm (least count of the screw gauge), the uncertainty in surface density will be  $2.71 \text{ g/cm}^3 \times 0.001 \text{ cm} = 2.71 \times 10^{-3} \text{ g/cm}^2$ .

Scatterer Thickness (mm)	Observed Counts		Avg. Count	Net Corrected Count
	I	II		
0.00	187	188	187.5	0.0
0.05	200	192	196	8.5
0.10	200	189	194.5	7.0
0.15	200	224	212	24.5
0.20	214	223	218.5	31.0
0.25	229	213	221	33.5
0.30	254	223	238.5	51.0
0.35	287	296	291.5	104.0
0.40	281	306	293.5	106.0
0.45	296	277	286.5	99.0

TABLE IV: Backscattering data for different scatterer thicknesses. The net corrected count is obtained by assuming the avg. count for 0mm scatterer thickness to be background data.

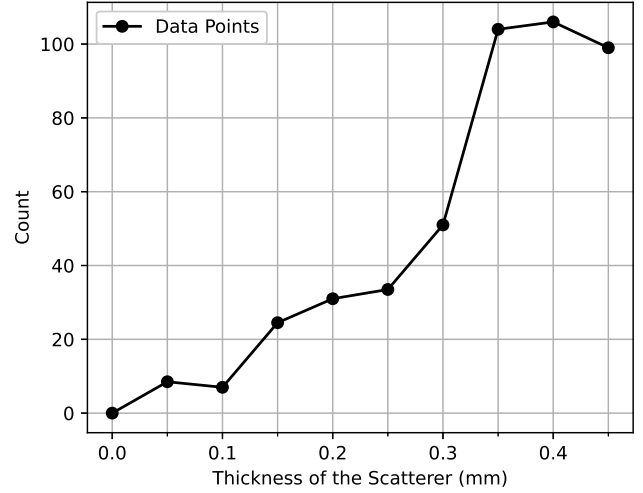


FIG. 6: Count vs. Scatterer thickness plot for Sr-204, from backscattering measurements

$$\Delta R_{Sr} = R_{Sr} \sqrt{\left( \frac{\Delta t_{\frac{1}{2}, Sr}}{t_{\frac{1}{2}, Sr}} \right)^2 + \left( \frac{\Delta t_{\frac{1}{2}, Tl}}{t_{\frac{1}{2}, Tl}} \right)^2}$$

$$= 0.060 \text{ g/cm}^2$$

Similarly, the uncertainty in the end-point energy will be,

$$\Delta E_{0, Sr} = E_{0, Sr} \left( \frac{\Delta R_{Sr}}{R_{Sr}} \right)$$

$$= 0.128 \text{ MeV}$$

Since we were only able to vary the thickness of the scatterer in the third part, the uncertainty in the saturation thickness is also the step size we used in the variation, i.e. 0.05 mm.

#### IV. DISCUSSION & CONCLUSION

Using the half-thickness method, the range of  $\beta$  particles from Sr-90 through an Aluminium absorber was measured to be  $(0.826 \pm 0.060)$  mg/cm<sup>2</sup>. The end point energy was measured to be  $(0.761 \pm 0.128)$  MeV. This was obtained by comparing the range of  $\beta$  particles from the Sr-90 source with a Tl-204 source whose end-point energy is known to us.

By studying the attenuation of Bremsstrahlung radiation by different combinations of Copper, Aluminium and Perspex, we found that more attenuation occurs when Perspex is facing the source. Conversely, we observed higher Bremsstrahlung counts when metals are facing the source. Among the metals, Copper was observed to show more counts than Aluminium, in line with the theory that the amount of Bremsstrahlung increases with the atomic number of the absorbing material.

We also studied backscattering, and observed that the count rate initially increases with an increase in scattering body thickness and eventually reaches saturation. The saturation thickness of Aluminium in our case was ob-

served to be  $(0.35 \pm 0.05)$  mm with a Sr-90  $\beta$ -source.

#### V. PRECAUTIONS AND SOURCES OF ERROR

1. The *dead time* of the GM counter, which is the time during which it cannot detect another event, might have led to a reduction in the count rate and an overestimation of the sample's activity.
2. Electronic noise produced by the components of the GM counter might have led to an increase in the count rate and an overestimation of the sample's activity.
3. We observe a high amount of fluctuation due to background noise, so to obtain accurate counts, a large number of observations are required.
4. The beta particles from the sample might have been absorbed by the GM tube's window, or the air between the sample and the GM counter.
5. Fluctuations in the GM counter's operating voltage might have led to changes in the count rate and an overestimation or underestimation of the sample's activity.

---

[1] *G.M. Counting System: User Manual*, Nucleonix Systems Pvt. Ltd. (2022).